Inorg. Chem. **1999,** *38,* 1596−1602

Binuclear Gd^{3+} Complex of a 34-Membered Macrocycle with Six Carboxymethyl Arms: X-ray Structures, Formation Constants, NMR, EPR, and ^{1}H NMR Relaxivities

Michiko B. Inoue,*[†,‡] Hisila Santacruz,[‡] Motomichi Inoue,[‡] and Quintus Fernando[†]

Department of Chemistry, University of Arizona, Tucson, Arizona 85721-0041, and CIPM, Universidad de Sonora, Hermosillo, Sonora 83000, Mexico

Received August 21, 1998

A 34-membered macrocyclic ligand with six pendant carboxymethyl groups has been synthesized by the coupling of two diethylenetriaminepentaacetate (dtpa) and two 1,4-diaminobutane units: the macrocycle is 2,12,19,29-tetraoxo-1,4,7,10,13,18,21,24,27,30-decaaza-4,7,10,21,24,27-cyclotetratriacontanehexaacetic acid, abbreviated as (34dtpabn)H$_6$. The macrocycle was crystallized as the acetone adduct (34dtpabn)H$_6$·2Me$_2$CO in the monoclinic space group $P2_1/n$ with $a = 14.566(2)$ Å, $b = 10.968(1)$ Å, $c = 16.133(2)$ Å, $\beta = 105.62(1)°$, and $Z = 2$. The acetone molecules have close contacts with some carbon atoms of the macrocycle. The protonation constants determined by potentiometric titration (0.1 M KCl, 25 °C) were log $K_1 = 9.70$ (standard deviation = 0.01), log $K_2 = 9.18$ (0.05), log $K_3 = 5.27$ (0.02), log $K_4 = 4.50$ (0.03), log $K_5 = 3.84$ (0.01), and log $K_6 = 3.23$ (0.01). The corresponding protonation sites were identified by the pD dependence of ^{1}H NMR shifts; the central amino nitrogen of each dtpa moiety has the highest basicity. The binuclear Gd^{3+} complex of the macrocycle was crystallized as the 2-propanol adduct [Gd$_2$(34dtpabn)(H$_2$O)$_2$]·2PrOH·7H$_2$O in the triclinic space group $P\bar{1}$ with $a = 11.880(1)$ Å, $b = 15.036(1)$ Å, $c = 17.396(1)$ Å, $\alpha = 94.986(5)°$, $\beta = 103.340(5)°$, $\gamma = 98.286(5)°$, and $Z = 2$. Each ligand molecule coordinates two Gd^{3+} ions forming a binuclear metal chelate with the Gd−Gd distance 10.8928(7) Å. The coordination geometry around each metal ion is a tricapped trigonal prism consisting of three carboxylate oxygens, two amide oxygens, three amino nitrogens, and a water oxygen. Propanol molecules are located near the macrocyclic cavity with some close C−C contacts shorter than the sum of the van der Waals radii of methyl and methylene groups. The logarithmic overall formation constants, log β(Gd$_p$LH$_r$), were determined by potentiometry (0.1 M KCl, 25 °C): for GdLH$_4$, 35.85 (estimated uncertainty = 0.21); GdLH$_3$, 33.89 (0.36); GdLH$_2$, 30.27 (0.07); GdLH, 25.59 (0.04); GdL, 16.46 (0.04); GdLH$_{-1}$, 4.93 (0.19); Gd$_2$L, 30.36 (0.33). Dipolar interaction operative between the two Gd^{3+} ions in the binuclear complex collapses the hyperfine structure in the EPR spectrum. The ^{1}H NMR relaxivities are enhanced as a result of the binuclear complex formation.

Introduction

Lanthanide macrocyclic compounds have attracted a great deal of interest because they have possible applications based on their magnetic and optical properties. One of the most important applications is the use of Gd^{3+} complexes for magnetic resonance imaging (MRI).[1,2] Nonionic Gd^{3+} complexes are potentially useful as MRI contrast agents with low toxicity.[3] For this reason, a number of macrocyclic ligands with pendant carboxylate groups have been synthesized, and the structures of their Gd^{3+} complexes have been studied extensively.[4] A family of dioxopolyazamacrocycles with pendant carboxymethyl groups have been reported to be synthesized in a single step by reactions between ethylenediaminetetraacetic (edta) dianhydride or diethylenetriaminepentaacetic (dtpa) dianhydride and aliphatic diamines.[5−10] The dtpa-derived macrocycles are represented by the general formula **1**, which has three amino groups, two amide groups, and three pendant carboxylate groups. The planarity of the amide groups defines the rigidity of the macrocyclic rings, and the unique arrangement of the three types of donor groups results in novel coordination properties.[7−15] Reaction between an acid dianhydride and a diamine also gives a (2:2)-cyclization product in which two acid anhydride and two diamine units are linked by four amide groups.[5,12,16] A binuclear Eu^{3+} complex with this type of dtpa-derived macrocycle **2a** has been studied by luminescence

---

[†] University of Arizona.

[‡] Universidad de Sonora.

(1) Lauffer, R. B. *Chem. Rev.* **1987**, *87*, 901.

(2) Aime, S.; Botta, M.; Fasano, M.; Terreno, E. *Chem. Soc. Rev.* **1998**, *27*, 19.

(3) Tweedle, M. F. *Invest. Radiol.* **1992**, *27*, S2.

(4) Alexander, V. *Chem. Rev.* **1995**, *95*, 273.

(5) Inoue, M. B.; Villegas, C. A.; Asano, K.; Nakamura, M.; Inoue, M.; Fernando, Q. *Inorg. Chem.* **1992**, *31*, 2480.

(6) Carvalho, J. F.; Kim, S.-H.; Chang, C. A. *Inorg. Chem.* **1992**, *31*, 4065.

(7) Inoue, M. B.; Inoue, M.; Muñoz, I. C.; Bruck, M. A.; Fernando, Q. *Inorg. Chim. Acta* **1993**, *209*, 29.

(8) Franklin, S. J.; Raymond, K. N. *Inorg. Chem.* **1994**, *33*, 5794.

(9) Inoue, M. B.; Navarro, R. E.; Inoue, M.; Fernando, Q. *Inorg. Chem.* **1995**, *34*, 6074.

(10) Inoue, M. B.; Oram, P.; Inoue, M.; Fernando, Q.; Alexander, A. L.; Unger, E. C. *Magn. Reson. Imaging* **1994**, *12*, 429.

(11) Inoue, M. B.; Inoue, M.; Fernando, Q. *Acta Crystallogr. C* **1994**, *50*, 1037.

(12) Frey, S. T.; Chang, C. A.; Carvalho, J. F.; Varadarajan, A.; Schultze, L. M.; Pounds, K. L.; Horrocks, W. DeW., Jr. *Inorg. Chem.* **1994**, *33*, 2882.

(13) Inoue, M. B.; Oram, P.; Inoue, M.; Fernando, Q. *Inorg. Chim. Acta* **1995**, *232*, 91.

(14) Inoue, M. B.; Oram, P.; Inoue, M.; Fernando, Q. *Inorg. Chim. Acta* **1996**, *248*, 231.

(15) Wu, S. L.; Franklin, S. J.; Raymond, K. N.; Horrocks, W. DeW., Jr. *Inorg. Chem.* **1996**, *35*, 162.

(16) Inoue, M. B.; Medrano, F.; Inoue, M.; Raitsimring, A.; Fernando, Q. *Inorg. Chem.* **1997**, *36*, 2335.

10.1021/ic981015p CCC: $18.00

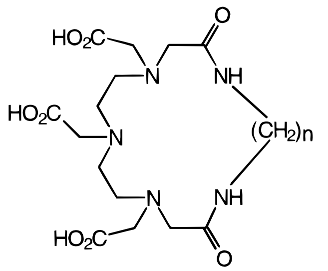

1a : n = 2
1b : n = 3
1c : n = 4
(17dtpabn)H_3

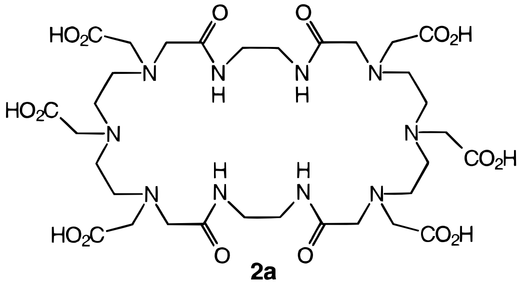

2a

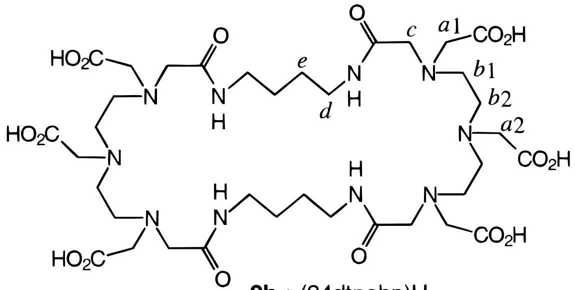

2b : (34dtpabn)H_6

spectroscopy and molecular mechanics.[12] The molecular mechanics calculations have suggested that the stable arrangement of three neighboring carboxylate arms is different from that of the mononuclear chelates of **1**.[12] These novel coordination properties of the dtpa-derived macrocycles have prompted us to study the X-ray structures of (2:2)-condensation macrocycles and their lanthanide metal complexes. In this work, we have synthesized a 34-membered macrocycle with two coordination centers (**2b**), abbreviated as (34dtpabn)H_6, and its binuclear Gd^{3+} complex, $[Gd_2(34dtpabn)(H_2O)_2]^0$, and we have determined their X-ray structures. Metal complex formation in solution was studied by potentiometric titrations. Since intramolecular interaction between two coordination centers in the binuclear complex is expected to influence the relaxation processes in magnetic resonance, the NMR relaxation times of the solvent water molecules were determined with the objective of evaluating the NMR relaxivities related to their ability to enhance the contrast in MRI.

Table 1. Crystallographic Data

	(34dtpabn)H_6·$2Me_2CO$	$[Gd_2(34dtpabn)(H_2O)_2]$·$2PrOH$·$7H_2O$
formula	$(C_{36}H_{62}N_{10}O_{16})\cdot 2(C_3H_6O)$	$Gd_2(C_{36}H_{56}N_{10}O_{16})\cdot 2(C_3H_7OH)\cdot 9(H_2O)$
fw	1007.11	1481.74
temp, °C	20	23
space group	$P2_1/n$ (No. 14)	$P\bar{1}$ (No. 2)
a, Å	14.566(2)	11.880(1)
b, Å	10.968(1)	15.036(1)
c, Å	16.133(2)	17.396(1)
α, deg	90	94.986(5)
β, deg	105.62(1)	103.340(5)
γ, deg	90	98.286(5)
V, Å^3	2482.0(5)	2968.6(7)
Z	2	2
ρ_{calc}, g cm^{-3}	1.35	1.66
μ, cm^{-1}	1.0	23.1
R [a]	0.049	0.039
R_w [b]	0.058	0.045

[a] $R = \Sigma|F_o - F_c|/\Sigma F_o$. [b] $R_w = [\Sigma w(F_o - F_c)^2/\Sigma wF_o^2]^{1/2}$.

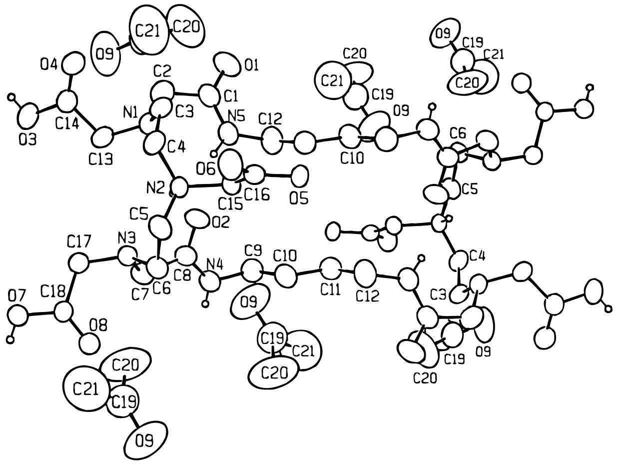

Figure 1. Structure of (34dtpabn)H_6·$2Me_2CO$. The macrocycle has an inversion center so that half the molecule is unique. Each macrocyclic molecule has close contacts with six surrounding acetone molecules, which are crystallographically equivalent. Least-squares planes (the range of deviations, Å): O2·N4·C7·C8·C9 (±0.05); O1·N5·C1·C2·C12 (±0.02). The non-hydrogen atoms are shown at the 50% probability level.

Results and Discussion

X-ray Structure of (34dtpabn)H_6·$2(C_2H_6CO)$. The acetone adduct of the macrocycle, (34dtpabn)H_6·$2Me_2CO$, crystallized from an aqueous solution containing acetone and did not contain any water of crystallization. The crystal data are summarized in Table 1. Figure 1 shows the molecular structure of (34dtpabn)H_6 and the surrounding acetone molecules. Selected interatomic distances are collected in Table 2. The molecular plane of the macrocyclic ring curves like an S. The hydrogen atoms H(N2), H(O3), and H(O7) were unequivocally located in the difference Fourier map. The central *N*-carboxymethyl group of each dtpa moiety is protonated on the nitrogen atom whereas two outer *N*-carboxymethyl groups are protonated on the carboxylate oxygen atoms. The protonation sites have been confirmed by the bond distances of non-hydrogen atoms: two C−O distances in each protonated carboxylate group differ by 0.103−0.111 Å, whereas the difference in an unprotonated CO_2 group is only 0.057 Å; the averaged N−C distance of the protonated amino nitrogen atom (N2) is 0.049 Å longer than the corresponding values of the unprotonated amino nitrogen atoms (N1 and N3), the N−C bonds of the protonated amino nitrogen atoms being weakened by donation of the lone pair electrons to a proton. The protonated carboxylate oxygen atoms (O3 and O7) form intermolecular hydrogen bonds (Table 2). On the other hand, the protonated amino nitrogen (N2) forms well-defined intramolecular hydrogen bonds with two amino nitrogen atoms (N1 and N3) and an amide oxygen atom (O2), stabilizing the S-shaped structure of the macrocycle molecule. With respect to the plane defined by three nitrogen donor atoms, N1, N2, and N3, the central carboxymethyl group and the hydrogen atom H(N2) are located on the same side, and the outer carboxymethyl groups protrude toward the opposite side. None of the carboxylate oxygen atoms form an intramolecular hydrogen bond with the protonated nitrogen, N2. This structural feature is quite different from that in the corresponding (1:1)-

Table 2. Selected Interatomic Distances (Å) and Angles (deg) for $(34dtpabn)H_6 \cdot 2Me_2CO$

Bond Distances

C1−O1	1.233(4)	C8−O2	1.235(3)
C14−O3	1.308(4)	C14−O4	1.197(4)
C16−O5	1.277(4)	C16−O6	1.220(5)
C18−O7	1.308(4)	C18−O8	1.205(4)
N1−C2	1.467(4)	N1−C3	1.448(5)
N1−C13	1.446(4)	N1−C (av)	1.454
N2−C4	1.502(4)	N2−C5	1.509(4)
N2−C15	1.498(4)	N2−C (av)	1.503
N3−C6	1.460(4)	N3−C7	1.448(5)
N3−C17	1.453(4)	N3−C (av)	1.454
N4−C8	1.312(5)	N4−C9	1.445(5)
N5−C1	1.323(4)	N5−C12	1.440(5)

Hydrogen Bonds

X−H(X)···Y	X−H(X)	X···Y	Y···H(X)	X−H(X)···Y
N2−H(N2)···N1	0.90(3)	2.967(4)	2.53(3)	110(2)
N2−H(N2)···N3	0.90(3)	2.853(3)	2.34(3)	116(2)
N2−H(N2)···O2	0.90(3)	2.993(4)	2.20(3)	147(3)
N5−H(N5)···O2	0.86(3)	2.898(3)	2.10(3)	155(3)
N5−H(N5)···N1	0.86(3)	2.776(4)	2.38(3)	109(2)
N4−H(N4)···O1′	0.73(3)	2.924(3)	2.22(3)	164(3)
O3−H(O3)···O5″	0.75(3)	2.634(3)	1.88(3)	173(3)
O7−H(O7)···O5′	0.74(3)	2.609(3)	1.88(3)	173(4)

Close Contacts of Acetone[a]

C20−C3	3.770(6)	C20−C4	3.845(5)
C20−C6′	3.858(6)	C21−C10″	3.948(7)
C21−C12″	4.004(6)	O9−C5″	3.338(5)
O9−C6″	3.155(5)		

[a] Interatomic distances equal to or less than the sum of the van der Waals radii. The van der Waals radius: O, 1.40 Å; CH_3, 2.0 Å; CH_2, 2.0 Å (ref 17).

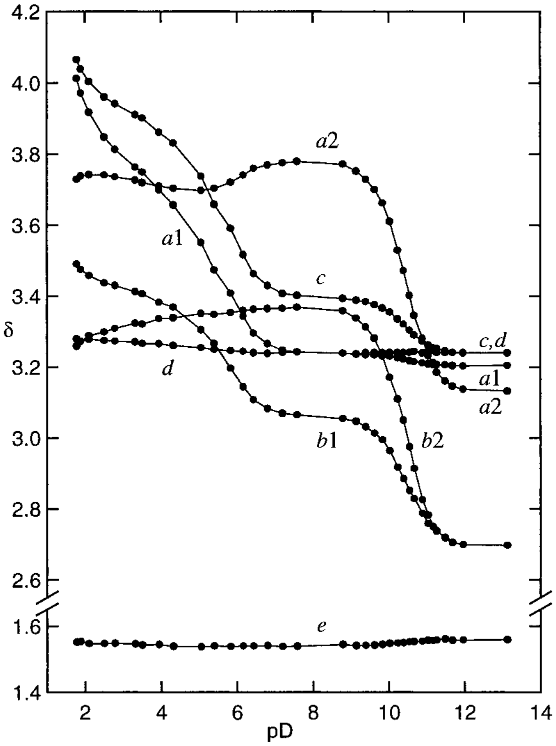

Figure 2. pD dependence of ^{1}H NMR shift δ (referenced to DSS) observed for $(34dtpabn)H_6$. For labeling, see formula **2b**. The *a*2 and *b*2 proton signals were broadened due to a sluggish exchange process at pD between 9 and 11.

macrocycle, $(17dtpabn)H_3$. In the latter molecule, three carboxymethyl groups protrude from the same side of the molecular plane, and an oxygen atom in the central *N*-carboxymethyl group forms an intramolecular hydrogen bond with the protonated nitrogen atom of the same group.[14]

Acetone molecules included in the adduct are difficult to liberate even in a vacuum at room temperature. Each solvent molecule has a number of close C−C and O−C contacts with three adjacent macrocyclic molecules. The interatomic distances shorter than the sum of the van der Waals radii are listed in Table 2.[17] The methyl carbons of acetone have close contacts with the dtpa moiety, rather than the butane moiety, of the macrocycle. Especially the methyl carbon C20 is very close to the methylene carbons C3, C4, and C6′ of the dtpa moieties. The methyl protons of acetone were unequivocally located in the difference Fourier map. This indicates that rotation of the methyl groups is hindered in a potential field defined by the neighboring macrocycle molecules, in contrast to usual methyl groups which undergo internal rotation about the C_3 axis. A fixed methyl group has a small effective volume in comparison with a rotating group and is able to approach closer to the adjacent molecules with a closer van der Waals contact. The acetone oxygen atom, O9, has close contacts with hydrophobic groups (C5 and C6) in the macrocycle and does not form hydrogen bonds with protonated carboxylate oxygens. These close C−O contacts suggest the presence of an O···H−C interaction.

Protonation of the Macrocycle in Solution. The protonation constants were determined by potentiometric titrations (0.1 M KCl, 25 °C) for $(34dtpabn)^{6-}$ as $\log K_1 = 9.70$ (standard deviation = 0.01), $\log K_2 = 9.18$ (0.05), $\log K_3 = 5.27$ (0.02), $\log K_4 = 4.50$ (0.03), $\log K_5 = 3.84$ (0.01), and $\log K_6 = 3.23$ (0.01). Figure 2 shows the ^{1}H NMR chemical shifts at different pD values. Only seven proton signals were observed throughout the pD range investigated; two protonation processes corresponding to K_1 and K_2 that occur on the chemically equivalent sites of two dtpa moieties cannot be distinguished by NMR titration; similarly, the other two pairs of protonation processes cannot be distinguished. In a pD range of 9−11, the CH_2 protons adjacent to amino nitrogens undergo a large downfield shift caused by the deshielding effect upon protonation processes corresponding to K_1 and K_2. The signal of the a2 proton (in formula **2b**) shifts back upfield with protonation in the pD range 5−7 and then very gradually shifts downfield again with a further decrease of pD. This pD dependence suggests that the protonation processes of K_3 and K_4 occur in the pD range 5−7, and those of K_5 and K_6 at pD below 5. These pD ranges of protonation are consistent with the $\log K_n$ values determined by potentiometry, when the difference between acid dissociation constants in H_2O and D_2O media is taken into account.[18]

The time-averaged proton populations $f_i(n)$ for each protonation step n (=1, 2, or 3) in half the macrocycle were calculated by the method reported previously[13,19] under the conditions $f_j(n) \leq 1$ and $f_{Nc}(n) + f_{Oc}(n) + 2[f_{No}(n) + f_{Oo}(n)] = n$, where Nc and Oc stand for the atoms of the central $>NCH_2CO_2^-$ group in a dtpa moiety, and No and Oo those of the outer groups. The calculated values are as follows: for $n = 1$ (i.e., LH_2^{4-} species), $f_{Nc}(1) = 0.85$, $f_{No}(1) = 0.06$, $f_{Oc}(1) = 0.03$, $f_{Oo}(1) = 0$; for $n = 2$ (LH_4^{2-}), $f_{Nc}(2) = 0.60$, $f_{No}(2) = 0.4_6$, $f_{Oc}(2) = 0.4_8$, $f_{Oo}(2) = 0$; for $n = 3$ (LH_6), $f_{Nc}(3) = 0.5$, $f_{No}(3) = 0.6_5$, $f_{Oc}(3) = 1.0$, $f_{Oo}(3) = 0.1$. The nitrogen Nc of the central

---

[17] Pauling, L. *The Nature of the Chemical Bond*, 3rd ed.; Cornell University Press: New York, 1960; p 261.

[18] Dean, J. A. *Lange's Handbook of Chemistry*, 13th ed.; McGraw-Hill: New York, 1985; Section 5, pp 14, 108.

[19] Sudmeier, J. L.; Reilley, C. N. *Anal. Chem.* **1964**, *36*, 1698.

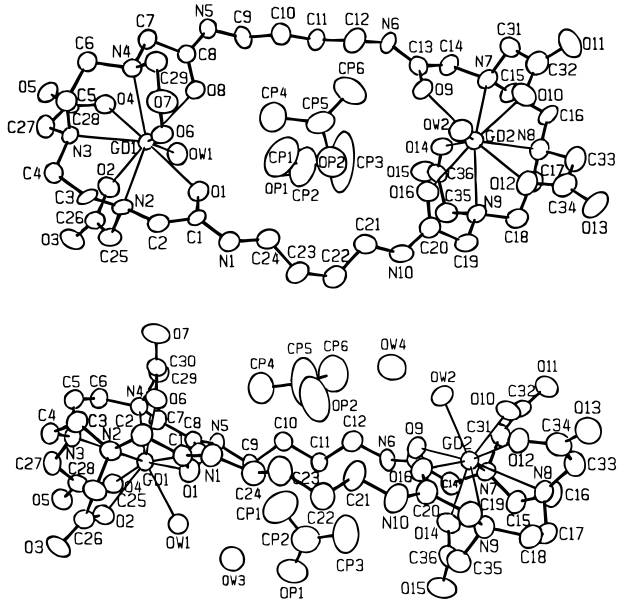

Figure 3. Molecular structure of $[Gd_2(34dtpabn)(H_2O)_2]{\cdot}2PrOH$ in top and side views; the side view includes two additional water oxygens, Ow3 and Ow4, that form hydrogen-bonding arrays with propanol oxygens (Op1 and Op2) and water oxygens (Ow1 and Ow2) coordinated to Gd atoms. The atoms are shown at the 50% probability level. Around the Gd1 atom, O1, O6, O8, O2, N3, and O4 form a distorted trigonal prism, the rectangular faces of which are capped by N2, N4, and Ow1; around the Gd2 atom, O14, O9, O16, N8, O10, and O12 form a trigonal prism, and N7, Ow2, and N9 reside above the rectangular faces. Least-squares planes (range of deviations, Å): for amide groups, O1·N1·C1·C2·C24 (±0.02), O8·N5·C7·C8·C9 (±0.04), O9·N6·C12·C13·C14 (±0.02), O16·N10·C19·C20·C21 (±0.05); for the diaminobutane group, N5·C9·C10·C11·C12·N6 (±0.06). Torsional angles in the other diaminobutane group: N10−C21−C22−C23, 172.1(8)°; C21−C22−C23−C24, 73(1)°; C22−C23−C24−N1, 169.7(8)°. Cp3 and Cp5 are disordered, and the averaged structures were determined for the propanol molecules. As a result, the bonding geometries around Cp2 and Cp5 were highly distorted from the regular tetrahedron.

$>NCH_2CO_2^-$ group in each dtpa moiety is mainly protonated at the step $n = 1$ and hence has a higher basicity than the nitrogen atoms of the outer $>NCH_2CO_2^-$ groups. This is consistent with the mode of protonation determined by the X-ray study in the solid state. The same mode of protonation has been reported for the corresponding (1:1)-macrocycle **1c**.[13,14] The protonation constant K_1 of $(34dtpabn)^{6-}$ is, however, significantly higher than that of $(17dtpabn)^{3-}$.[6,13] The higher basicity of the amino nitrogen in the 34-membered macrocycle results from the larger ring size.[20] Protonation in the step $n = 2$ occurs on No and Oc. The protons are, however, redistributed and shared almost equally by the protonated atoms so that electrostatic repulsion is minimized. As a result, the proton population on Nc is decreased, leading to the reverse shifts of H*a*2 and H*b*2 with the second protonation. A similar reverse shift with protonation has been reported for macrocycles **1a**, **1b**, **1c**, and dtpa.[13,21,22] In the fully protonated species, $(34dtpabn)H_6$, Oc is almost fully protonated, whereas the population on Oo is very small. The proton distribution of $(34dtpabn)H_6$ in solution is different from that in the solid state. In solution, protons can be exchanged rapidly between donor atoms and form intramolecular hydrogen bonds.[23] In the solid state, protons are bonded to donor atoms so as to minimize the lattice energy as well as the energies of the participating molecules.

Table 3. Selected Interatomic Distances (Å) for $[Gd_2(34dtpabn)(H_2O)_2]{\cdot}2PrOH{\cdot}7H_2O$

Gd−X Distances			
Gd1−O1	2.420(6)	Gd2−O9	2.430(6)
Gd1−O2	2.374(6)	Gd2−O10	2.341(6)
Gd1−O4	2.407(5)	Gd2−O12	2.396(6)
Gd1−O6	2.344(6)	Gd2−O14	2.343(6)
Gd1−O8	2.456(6)	Gd2−O16	2.409(6)
Gd1−N2	2.667(6)	Gd2−N7	2.683(6)
Gd1−N3	2.636(7)	Gd2−N8	2.633(8)
Gd1−N4	2.697(7)	Gd2−N9	2.801(7)
Gd1−Ow1	2.463(7)	Gd2−Ow2	2.438(7)
Gd1−Gd2	10.8928(7)		
Close Contacts of Propanol[a]			
Cp1−Cp4	4.13(2)	Cp1−C24	3.75(2)
Cp2−C22′	4.04(2)	Cp3−C22′	3.92(3)
Cp3−C35	4.06(2)	Cp3−C36	3.52(2)
Cp4−C1	4.18(2)	Cp4−C29	4.09(2)
Cp4−C30	3.65(2)	Cp5−C15′	4.19(2)
Cp6−C10′	4.04(2)	Cp6−C12	3.91(2)
Cp6−C29′	3.83(2)		
Op1−Ow3	2.74(1)	Op2−Ow4	2.84(1)
Ow3−Ow1	2.92(1)	Ow4−Ow2	2.811(9)

[a] C−C distances less than 4.2 Å and O−O distances with hydrogen bonds. The van der Waals radius: C, 1.70 Å; CH_3, 2.0 Å; CH_2, 2.0 Å (ref 17).

X-ray Structure of $[Gd_2(34dtpabn)(H_2O)_2]{\cdot}2PrOH{\cdot}7H_2O$. The 34-membered macrocycle formed a binuclear Gd^{3+} complex, which crystallized as a 2-propanol adduct with water of crystallization. Figure 3 shows the molecular structure of $[Gd_2(34dtpabn)(H_2O)_2]{\cdot}2PrOH$. Selected interatomic distances are collected in Table 3. Two Gd atoms in a $[Gd_2(34dtpabn)(H_2O)_2]$ molecule have resembling modes of coordination, although they are crystallographically independent. Each Gd atom is coordinated to three amino nitrogens, two amide oxygens, three carboxylate oxygens, and a water oxygen. The resulting nine-coordination geometry can be described as a distorted tricapped trigonal prism. The Gd−X distances in each coordination sphere are in the order Gd−N(amino) > Gd−O(water) ≥ Gd−O(amide) > Gd−O(carboxylate). This trend is the same as in $[Gd(17dtpabn)(H_2O)]^0$.[10] The central metal ions in $[Gd_2(34dtpabn)(H_2O)_2]^0$ are located slightly out of the macrocyclic plane. With respect to this plane, two neighboring carboxylate groups in half the metal chelate molecule are located on the same side as the metal ion to which they are coordinated, whereas the third coordinated carboxylate group is located on the opposite side. This up−up−down arrangement of the carboxylate arms with respect to the molecular plane of the macrocyclic ligand differs from the up−up−up arrangement in $[Gd(17dtpabn)(H_2O)]^0$; the latter arrangement has been commonly reported for a number of mononuclear lanthanide complexes of polyazamacrocycles with three neighboring *N*-carboxymethyl arms, such as **1b**, DO3A (1,4,7,10-tetraazacyclododecane-*N*,*N*′,*N*″-triacetic acid), and DO3A derivatives.[7−10,24−27]

---

(20) Inoue, M. B.; Medrano, F.; Inoue, M.; Fernando, Q. *J. Chem. Soc., Perkin Trans. 2* **1998**, 2275.

(21) Kula, R. J.; Sawyer, D. T. *Inorg. Chem.* **1964**, *3*, 458.

(22) Letkeman, P.; Martell, A. E. *Inorg. Chem.* **1979**, *18*, 1284.

(23) Desreux, J. F.; Merciny, E.; Loncin, M. F. *Inorg. Chem.* **1981**, *20*, 987.

(24) Aime, S.; Anelli, P. L.; Botta, M.; Fedeli, F.; Grandi, M.; Paoli, P.; Uggeri, F. *Inorg. Chem.* **1992**, *31*, 2422.

(25) Kang, L. I.; Ranganathan, R, S.; Emswiler, J. E.; Kumar, K.; Gougoutas, J. Z.; Malley, M. F.; Tweedle, M. F. *Inorg. Chem.* **1993**, *32*, 2912.

(26) Chang, C. A.; Francesconi, L. C.; Malley, M. F.; Kumar, K.; Gougoutas, J. Z.; Tweedle, M. F.; Lee, D. W.; Wilson, L. J. *Inorg. Chem.* **1993**, *32*, 3501.

(27) Kumar, K.; Chang, C. A.; Francesconi, L. C.; Dischino, D. D.; Malley, M. F.; Gougoutas, J. Z.; Tweedle, M. F. *Inorg. Chem.* **1994**, *33*, 3567.

A molecular mechanics calculation performed on the binuclear Eu^{3+} complex of **2a** has shown that the up−down−up arrangement is stable compared with other arrangements in this complex.[12] The same type of arrangement is formed in the uncoordinated ligand **2b**, but its Gd^{3+} complex has the up−up−down arrangement. The opposite orientation of one arm to the other two (i.e., in the up−up−down or up−down−up arrangement) may decrease steric constraints in the binuclear complexes, unlike in the mononuclear complexes. It is not clear, however, whether the difference between the arrangements in Eu_2−**2a** and Gd_2−**2b** is caused by the nature of the ligands (such as ring size) or by other factors (such as the effect of crystallization and the assumptions made in the molecular mechanics calculation).

One of the interesting structural features of the binuclear Gd^{3+} complex is that 2-propanol molecules are located close to the macrocyclic cavity, and partially encapsulated, in contrast to the acetone adduct of the uncoordinated ligand in which acetone molecules are located outside the macrocyclic cavity (Figure 1). The averaged molecular plane of the non-hydrogen atoms in one propanol molecule is parallel to the plane of the macrocycle, and the other propanol molecule is perpendicular. Two propanol molecules that reside on either side of the macrocyclic plane are in van der Waals contact with the short Cp1−Cp4 distance (Table 3). The alcohol oxygens are indirectly anchored on the metal chelate via hydrogen-bonding arrays, Op1−Ow3−Ow1−Gd1 and Op2−Ow4−Ow2−Gd2. Some short carbon−carbon distances are present between propanol and the hydrophobic butane moiety of the macrocyclic molecule (Table 3). The C−C contacts, together with the hydrogen-bonding arrays, result in the partial encapsulation of propanol molecules. The coordination of the pendant carboxylate groups to the metal ions leaves large vacancies above and below the plane of the macrocycle. Filling the vacancies with specific organic molecules is supposedly essential for crystallization of the complex. In fact, slow concentration of aqueous solutions (without the addition of 2-propanol or ethanol) gave only vitreous solids, and the addition of acetone to an aqueous solution gave a powdery precipitate, the elemental analyses of which showed that no acetone was present.

Formation Constants. The formation constants were determined by potentiometric titrations in the concentration ratios $[Gd^{3+}]/[(34dtpabn)^{6-}] = 1$ and 2 in 0.1 M KCl media at 25 °C. The logarithmic overall formation constants, $\log \beta(Gd_pLH_r) = \log [Gd_pLH_r]/[Gd]^p[L][H]^r$, were as follows: for $GdLH_4$, 35.85 (estimated uncertainty = 0.21); $GdLH_3$, 33.89 (0.36); $GdLH_2$, 30.27 (0.07); GdLH, 25.59 (0.04); GdL, 16.46 (0.04); $GdLH_{-1}$, 4.93 (0.19); Gd_2L, 30.36 (0.33) (the species distributions are shown in Figure S1 in Supporting Information). In the [Gd]/[L] = 1 system, a number of $GdLH_n$ species are formed in which donor atoms in the vacant coordination site are protonated. The major species in the neutral region is GdLH, and the GdL species has a maximum concentration at pH ≈ 10.5; $\log [GdLH]/[GdL][H] = 9.13$ is practically identical with $\log K_2$ of the free ligand. The logarithmic formation constant 16.46 of GdL is larger than 15.39 reported for Gd−(17dtpabn), and close to 16.85 of a Gd complex with an acyclic bisamide derivative of dtpa,[6] as predicted from the protonation constants of the amino nitrogen in these ligands. This is probably a result of the high flexibility of the 34-membered ring. In the [Gd]/[L] = 2 system, the Gd_2L species forms in 100% yield at pH > 4, while the [Gd]/[L] = 1 system contains the Gd_2L species in considerable concentration; in a solution of [Gd] = [L] = 1 mM at pH = 7, GdLH ≈ 81% and $Gd_2L \approx LH_2 \approx 9\%$.

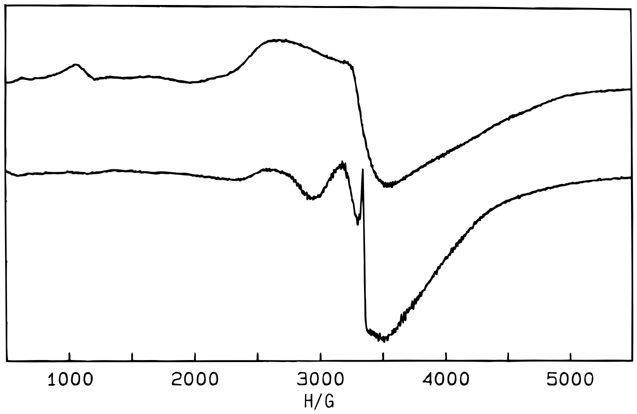

Figure 4. EPR spectra of $[Gd_2(34dtpabn)]^0$ (top) and $[Gd(17dtpabn)]^0$ (bottom) in a 50% methanol glass matrix with an approximate Gd concentration of 10^{-2} M at 4.2 K. The resonance frequency was 9.3455 GHz.

EPR Spectra. Figure 4 shows the EPR spectra observed for $[Gd_2(34dtpabn)]^0$ and the corresponding mononuclear complex $[Gd(17dtpabn)]^0$ in 50% methanol glass matrixes at 4.2 K; essentially the same spectral patterns were observed at 78 K. The mononuclear complex exhibited an ill-defined structure arising from the electron spin−nuclear spin coupling ($I_{Gd} = {}^7/_2$). For the binuclear complex, the hyperfine structure was not observed at all. The paramagnetic moment of one Gd^{3+} ion ($S = {}^7/_2$) in a $[Gd_2(34dtpabn)(H_2O)_2]^0$ molecule produces a dipolar field on the other paramagnetic site. The field strength is calculated as $\mu/r^3 = 57$ G on the basis of the Gd−Gd distance 10.8928(7) Å in the solid state: the dipolar interaction energy μ^2/r^3 is 4.2×10^{-25} J. This dipolar interaction collapses the hyperfine structure in the EPR spectrum.

Absorption and Fluorescence Spectra of Eu^{3+} Complex. Gadolinium(III) complexes are usually isostructural with the corresponding Eu^{3+} complexes, whose absorption and fluorescence spectra have been extensively studied.[28−31] The absorption spectra of solutions containing Eu^{3+} and $(34dtpabn)H_6$ in the ratios [Eu]/[L] = 1 and 2 at pH = 7.5 showed an intense absorption band at 395 nm together with weak bands at 362, 366, 376, 381, 384, 398, and 465 nm; this spectral pattern is identical with that observed for $[Eu(17dtpabn)]^0$ and that reported for $[Eu(dtpa)]^{2-}$,[28] except that an absorption envelope extending from the UV to the visible region was more intense in the Eu_n−(34dtpabn) solutions (Figure S2 in Supporting Information). Fluorescence spectra were recorded for the above sample solutions with a conventional spectrofluorometer, although its resolution was not high enough to observe the sharp luminescence lines of Eu^{3+} complexes. The Eu−(34dtpabn), Eu_2−(34dtpabn), and Eu−(17dtpabn) solutions showed emission bands centered at 590 nm ($^5D_0 \rightarrow {}^7F_1$) and 615 nm ($^5D_0 \rightarrow {}^7F_2$) with excitation at 395 nm. The excitation spectrum observed for the 615 nm emission of the [Eu]/[34dtpabn] = 1 solution had a well-defined band at 390 nm which was identical with that observed for the Eu−(17dtpabn) complex and that reported for the Eu−(dtpa) complex,[28−30] whereas the [Eu]/[34dtpabn] = 2 solution showed only an ill-defined shoulder at 390 nm on an envelope extending from the UV region. This observation suggests that the relaxation process related to the fluorescence is influenced by binuclear complex formation.

---

(28) Gallagher, P. K. *J. Chem. Phys.* **1964**, *41*, 3061.
(29) Bryden, C. C.; Reilley, C. N. *Anal. Chem.* **1982**, *54*, 610.
(30) Albin, M.; Horrocks, W. DeW., Jr. *Inorg. Chem.* **1985**, *24*, 895.
(31) Horrocks, W. DeW., Jr.; Sudnick, D. R. *J. Am. Chem. Soc.* **1979**, *101*, 334.

NMR Relaxivities. The ^{1}H NMR relaxation times T_1 and T_2 of water molecules were determined in aqueous 90% D_2O solutions of the binuclear Gd^{3+} chelate, $[Gd_2(34dtpabn)(H_2O)_2]^0$, at pH = 6.9 and at a resonance frequency of 250 MHz. The relaxivities r_1 and r_2 per Gd were calculated by $T_n^{-1} = r_n[Gd] + T_{n0}^{-1}$ where $n = 1$ or 2 and $T_{n0} = T_1$ or T_2 at [Gd] = 0. The species distribution curves calculated with the formation constants indicate that free Gd^{3+} ions dissociated from $[Gd_2(34dtpabn)(H_2O)_2]^0$ are negligible at pH = 6.9 in the concentration range 1−5 mM (per Gd) suitable for relaxivity measurements. The [Gd]/[L] ratio in the sample solutions was, however, set to 2/1.05, to ensure the absence of free Gd^{3+} ions, because free Gd^{3+} ions yield a very large error owing to their relaxivities that are much higher than those of common Gd^{3+} chelates.[1] The relaxivities per Gd were determined as $r_1 = 4.9$ mM^{-1} s^{-1} and $r_2 = 6$ mM^{-1} s^{-1}. These values are in the range of values reported for Gd^{3+} complexes used in MRI diagnosis such as Gd−DO3A.[25,32] A quantitative comparison can be made only for the values determined under identical experimental conditions, because the relaxivities are influenced by a number of factors including magnetic resonance frequency and D_2O concentration[1,2] (since an NMR spectrometer for chemical characterization was employed in this work, D_2O was required as an internal lock). For $[Gd(17dtpabn)(H_2O)]^0$, the relaxivities have been determined as $r_1 = 3.4$ mM^{-1} s^{-1} and $r_2 = 4.0$ mM^{-1} s^{-1} under the same experimental conditions as in this work.[10] Similar values were reported for the mononuclear Gd^{3+} complexes of 16-membered analogues under the same experimental conditions.[9,10] The relaxivities per Gd of $[Gd_2(34dtpabn)(H_2O)_2]^0$ are significantly higher than the corresponding values of $[Gd(17dtpabn)(H_2O)]^0$. Since only 5% of the Gd_2L species are converted to GdLH by the excess ligand, the observed high relaxivities are ascribable to the binuclear complex. It has been reported that, when two $[Gd(DO3A)(H_2O)]^0$ units are linked, the resulting binuclear chelate has a 36% higher r_1 than the mononuclear chelate, as a result of an increase in the rotational correlation time due to the larger molecular weight and size.[33] This molecular size effect is certainly present in $[Gd_2(34dtpabn)(H_2O)_2]^0$. For this binuclear complex, additional factors which enhance the relaxivities are conceivable. For example, the dipolar interaction between two Gd^{3+} ions in a binuclear molecule modulates the magnetic field in the vicinity of the chelate molecule. This field modulation may shorten the NMR T_2 of surrounding water molecules and consequently enhance the relaxivity r_2. The binuclear complex formation also may accelerate geometrical fluctuation of the coordination sphere such as the exchange of a coordinated water molecule with solvent molecules. This results in the higher r_1 value. In conclusion, this work suggests that binuclear complex formation is a new approach to the synthesis of a highly efficient MRI contrast enhancer.

Experimental Section

Syntheses. To 2.5 g of dtpa dianhydride (Sigma) suspended in 300 mL of dimethylformamide (DMF) was added 0.75 mL of 1,4-diaminobutane (Aldrich) in 60 mL of DMF dropwise with vigorous stirring under a nitrogen atmosphere. The colorless solid formed was removed by filtration. The filtrate was concentrated to a yellow oil. Addition of tetrahydrofuran gave a colorless solid. Recrystallization of this crude product from a small amount of water gave pure $(17dtpabn)H_3$ with a yield of 40%.[10] When further concentration gave a slightly viscous liquid without forming any crystals, the mother liquor was mixed with the same amount of acetone. In a few days, $(34dtpabn)H_6$ crystallized as the acetone adduct, and some crystals were found to be suitable for X-ray crystal analyses. The use of other common organic solvents as a precipitant instead of acetone gave $(34dtpabn)H_6$ as powdery precipitates that contained open chain oligomers as main contaminants. When acetone was used instead of tetrahydrofuran as a precipitant for the crude product, separation with a Sephadex G-10 (Sigma) column was required; the first eluate, obtained by using deionized water as an eluent and a conductance meter as a monitor of the effluent, was concentrated and mixed with acetone to give the acetone adduct of $(34dtpabn)H_6$. The product was recrystallized from water/acetone and dried in a vacuum at room temperature. Yield: 13%. Mp: 176−179 °C dec. Anal. Calcd for $C_{36}H_{62}N_{10}O_{16}\cdot 2(C_3H_6O)$: C, 50.09; H, 7.41; N, 13.91. Found: C, 49.72; H, 7.39; N, 14.07 (the elemental analyses were performed by Desert Analytics, Tucson, AZ). ^{1}H NMR (D_2O, pD = 3.5, referenced to DSS): δ = 1.54 (8H, unresolved t, assigned to H*e* in formula **2b**), 3.27 (8H, unresolved t, H*d*), 3.32 (8H, unresolved t, H*b2*), 3.41 (8H, unresolved t, H*b1*), 3.72 (4H, s, H*a2*), 3.75 (8H, s, H*a1*), 3.90 (8H, s, H*c*). ^{13}C NMR (D_2O, pD = 3.5, 62.9 MHz, DSS): δ = 28.4 (C*e*); 41.7(C*d*), 54.1 and 54.3 (C*b1*, C*b2*), 57.0 (C*a2*), 59.3 and 59.8 (C*a1*, C*c*), 171.1 and 175.0 (CO_2^-), 174.8 (CONH); the signals were assigned on the basis of their pD dependence.

The Gd^{3+} complex was prepared by a reaction between the ligand and excess Gd^{3+} carbonate (Johnson Matthey) in a small amount of water at approximately 40 °C. The unreacted carbonate was removed by filtration. Addition of acetone to the filtrate yielded $Gd_2(C_{36}H_{56}N_{10}O_{16})\cdot 9H_2O$ as a colorless solid. Anal. Calcd: C, 31.75; H, 5.48; N, 10.29. Found: C, 31.50; H, 5.18; N, 10.14. 2-Propanol was diffused into a dilute solution of the Gd^{3+} complex in a small-bore tube so that fine crystals were formed in several days. With a very slow concentration of this mixture, crystals of the 2-propanol adduct suitable for X-ray analyses were obtained after several months.

X-ray Crystal Analyses. The single-crystal X-ray analyses of the macrocycle and its Gd^{3+} complex were performed with monochromated Mo Kα radiation ($\lambda = 0.710\,73$ Å) on an Enraf-Nonius CAD4 diffractometer. Scattering factors were taken from Cromer and Waber.[34] All calculations were performed on a VAX computer with the program package MolEn.[35]

A colorless platelike crystal of $(34dtpabn)H_6\cdot 2(C_3H_6O)$ with approximate dimensions of 0.45 × 0.27 × 0.12 mm was mounted on a glass fiber. The crystal system was monoclinic (Table 1). A total of 4787 reflections ($+h,+k,\pm l$) with a maximum 2θ of 50° were collected; 4354 reflections were unique; 2329 reflections with $I > 3\sigma_I$ were used in the refinements. No absorption correction was made. The structure was solved by direct methods, and 34 atoms were located from an *E* map. The remaining atoms were located in succeeding difference Fourier syntheses. A $(34dtpabn)H_6$ molecule had an inversion center so that half the molecule was unique. Near the amino nitrogen atom N2 and carboxylate oxygen atoms O3 and O7, peaks attributable to hydrogen atoms were located in the difference Fourier map. These hydrogen peaks were refined isotropically with a fixed temperature factor of 5.0 Å^2, and the presence of the hydrogen atoms was confirmed. The amide hydrogen atoms were also refined, and the other hydrogen atoms of the macrocycle were placed at the idealized positions. The hydrogen atoms of acetone were located in the difference Fourier map and included in the refinement as riding atoms. The final refinement converged at $R = 0.049$ with 331 parameters. The maximum and minimum peaks in the final difference map were 0.19(4) and −0.08(4) e Å^{-3}, respectively.

A colorless crystal of $[Gd_2(34dtpabn)(H_2O)_2]\cdot 2PrOH\cdot 7H_2O$ with approximate dimensions 0.33 × 0.17 × 0.08 mm was sealed in a capillary with the mother liquor. The crystal system was triclinic; 10 410 unique reflections ($+h,\pm k,\pm l$) with a maximum 2θ of 50° were

---

(32) Zhang, X.; Chang, C. A.; Brittain, H. G.; Garrison, J. M.; Telser, J.; Tweedle, M. F. *Inorg. Chem.* **1992**, *31*, 5597.

(33) Toth, E.; Vauthey, S.; Pubanz, D.; Merbach, A. E. *Inorg. Chem.* **1996**, *35*, 3375.

(34) Cromer, D. T.; Waber, J. T. *International Tables for X-ray Crystallography*; The Kynoch Press: Birmingham, England, 1974; Vol. IV, Table 2.2B.

(35) Fair, C. K. *MolEn. An Interactive Intelligent System for Crystal Structure Analysis*; Enraf-Nonius: Delft, The Netherlands, 1990.

collected; 5682 reflections with $I > 3\sigma_I$ were used in the refinements. An empirical absorption correction based on six ψ-scans was applied using the program PSICALC. Relative transmission coefficients ranged from 0.792 to 1.000. The positions of two Gd atoms were located by the Patterson heavy-atom method. The remaining non-hydrogen atoms were located in succeeding difference Fourier syntheses. All the constituent atoms of propanol have relatively large thermal parameters: the equivalent isotropic displacement parameters, B_{eq}, are in the range 7.5(3)−17.0(6) Å^2. Moreover, the displacement factors of Cp3 and Cp5 are highly anisotropic. This suggests that these carbon atoms are disordered between equivalent positions. Such a disorder, however, was not modeled, and the averaged structure was determined. For this reason, the bonding geometries around the secondary carbon atoms, Cp2 and Cp5, were highly distorted from the regular tetrahedron. The hydrogen atoms of the ligand molecule were placed at the idealized positions. Ten water hydrogen atoms were located in a difference Fourier map and included in the refinement as riding atoms. Other water hydrogen and propanol hydrogen atoms, which could not be located, were not included in the refinement. The final refinement converged at $R = 0.039$ with 730 parameters. The maximum and minimum peaks in the final difference map were 1.56(12) and −0.18(12) e Å^{-3}, respectively, large peaks being located around the Gd atoms.

Potentiometric Titrations. Potentiometric titrations were carried out by the use of a piston-type buret in an aqueous KCl medium at an ionic strength of 0.1 and a controlled temperature of 25 °C under a nitrogen atmosphere. The pH values were determined by a Beckman Phi-72 pH meter equipped with Ross glass and reference electrodes. A 0.1 M KOH solution was prepared by dissolving ACS-certified KOH (Mallinckrodt) in water boiled and cooled under nitrogen flow, and standardized with potassium hydrogen phthalate (Fisher). A 0.1 M HCl (Ricca) solution restandardized with Na_2CO_3 (Aldrich) was titrated with the standardized 0.1 M KOH solution at an ionic strength of 0.1, and the calculated H^+ concentrations were used to convert the pH meter readings to $-\log [H^+]$. A Gran plot was used to estimate the extent of carbonate contamination of the base, which was less than 1%. The exact concentration of a stock solution of the ligand was determined by titration with the standard 0.1 M KOH, and the acid dissociation constants were calculated by the use of the program PKAS.[36] A 0.01 M stock solution of Gd^{3+} was prepared from gadolinium chloride (Johnson Matthey) and standardized by edta titration. Titrations for determination of the formation constants were carried out for [Gd]/[L] = 1 and 2 with 0.05 mmol of ligand in an initial volume of 50 mL; for [Gd]/[L] = 2, a slight excess of ligand was used to prevent precipitation of hydroxide. About 80 data points were collected for each titration. A slow equilibrium was observed for 3−4 points in the unbufferd region; the longest time required for reaching equilibrium was 15 min for [Gd]/[L] = 1 and 1 h for [Gd]/[L] = 2. Except for these points, equilibrium was reached within 5 min, and each titration could be performed during the time in which the drift of the measuring system was tolerable. All calculations were performed by using the program BEST.[36]

Spectroscopic and Magnetic Measurements. The ^1H NMR spectra were obtained with a Bruker AM 250 spectrometer at a probe temperature of approximately 23 °C. The internal reference was sodium 2,2-dimethyl-2-silapentane-5-sulfonate, DSS (Aldrich). The pH value of each sample solution was measured with an Aldrich long-stem combination electrode, which was calibrated with standard aqueous buffers (Fisher). The measured pH values were converted to pD values by $pD = pH_{measd} + 0.44$.[37] A minimum quantity of dilute KOD solution or dilute DCl was used for adjusting pD.

The EPR spectra were obtained on a Bruker ESP-300 X-band EPR spectrometer for the Gd^{3+} complexes in a 50% methanol glass matrix; the concentration was approximately 10 mM per Gd. The absorption and emission spectra of the Eu^{3+} chelate were obtained on a Perkin-Elmer Lambda 2 UV−vis spectrometer and on a JASCO 821-FP spectrofluorometer at a temperature of ≈25 °C.

The ^1H NMR relaxation times T_1 and T_2 were determined with a Bruker AM 250 spectrometer for aqueous 90% (v/v) D_2O solutions containing the binuclear chelate at 250 MHz and a probe temperature of 23 °C. The $180°-\tau-90°$ pulse sequence technique was used for T_1 measurements, and the Carr−Purcell−Meiboom−Gill method for T_2.[38] A stock solution was prepared in the concentration ratio [Gd]/[L] = 2/1.05 from a standardized Gd^{3+} solution and precisely weighed $(34dtpabn)H_6{\cdot}2Me_2CO$. The pH value (without correction for D_2O) was adjusted to 6.9 by adding solid $NaHCO_3$. The sample solutions were prepared from the stock solution in the concentration range 1−5 mM per Gd.

Acknowledgment. We thank Arnold Raitsimring for performing the EPR measurements.

Supporting Information Available: Species distribution curves for [Gd]/[34dtpabn] = 1 and 2 and the absorption spectra of Eu−(34dtpabn) and Eu_2−(34dtpabn) solutions. Two X-ray crystallographic files for $(34dtpabn)H_6{\cdot}2Me_2CO$ and $[Gd_2(34dtpabn)(H_2O)_2]{\cdot}2PrOH{\cdot}7H_2O$ are available in CIF format. This material is available free of charge via the Internet at http://pubs.acs.org.

IC981015P

---

(36) Martell, A. E.; Motekaitis, R. J. *Determination and Use of Stability Constants*, 2nd ed.; VCH Publishers: New York, 1992.

(37) Mikkelsen, K.; Nielsen, S. O. *J. Phys. Chem.* **1960**, *64*, 632.

(38) Farrar, T. C.; Becker, E. D. *Pulse and Fourier Transform NMR, Introduction to Theory and Methods*; Academic Press: New York, 1971.